Palaeogeography, Palaeoclimatology, Palaeoecology 490 (2018) 629–639

Contents lists available at ScienceDirect

Palaeogeography, Palaeoclimatology, Palaeoecology

journal homepage: www.elsevier.com/locate/palaeo

Penguin colonization following the last glacial-interglacial transition in the Vestfold Hills, East Antarctica

Yuesong Gao[a], Lianjiao Yang[a], Jianjun Wang[b,*], Zhouqing Xie[a,*], Yuhong Wang[a], Liguang Sun[a,*]

[a] Institute of Polar Environment & Anhui Key Laboratory of Polar Environment and Global Change, School of Earth and Space Sciences, University of Science and Technology of China, Hefei 230026, China

[b] Key Laboratory of Global Change and Marine-Atmospheric Chemistry, Third Institute of Oceanography, State Oceanic Administration, Xiamen, China

ARTICLE INFO

Keywords:
Penguin occupation
Population reconstruction
Ornithogenic sediment
Deglaciation
Ice retreat
Penguin-derived proxies

ABSTRACT

The population history of the Adélie penguin (*Pygoscelis adeliae*) and its response to climatic and environmental changes have been widely studied in maritime Antarctica and several glacial refugia of Adélie penguins were dated back to the Last Glacial Maximum. However, the process of colony expansion during the subsequent glacial-interglacial transition was less well-documented. In this paper, we investigate an ornithogenic core from Vestfold Hills, East Antarctica, to improve knowledge of postglacial penguin colonization. Local deglaciation occurred around 15.6 kyr BP, based on a coarse-grained detrital layer, a date that is earlier than most of those reported in other studies from the same region. Geochemical analysis of the core suggests penguins started colonizing the northern Vestfold Hills around 14.6 kyr BP, the oldest geological record in East Antarctica on penguin occupation, and their population exhibited a broadly increasing trend thereafter. The population expanded at approximately 6740 yr BP, in the mid-Holocene, which corresponds to a local climatic optimum. Although this inference is based on population changes of local sub-colonies, it corresponds well to reconstructions of regional climate change, and changes in the penguin population based on genetic studies. From a consideration of the results of previous studies of the occupation history of sea birds following deglaciation in the Arctic, as well as other parts of Antarctica, we propose that sea birds colonized the emerging ice-free areas shortly after local glacier retreat. Over geological time-scales, the availability of breeding habitat is a key factor controlling the population size and activity range of Antarctic Adélie penguins.

1. Introduction

The Vestfold Hills (68° 33′ S, 78° 15′ E), Prydz Bay, is one of the most important ice-free areas in East Antarctica (Fig. 1, Mackintosh et al., 2014), and its Holocene climate history has been widely studied. During the early Holocene, regions of the Vestfold and Larsemann Hills (69° 24′ S, 76° 13′ E) experienced the 'early-Holocene optimum' from 11.5–9.5 kyr BP (thousand years before 1950 CE), when the climate was warm and humid, as inferred from lake sediment records (Verleyen et al., 2004, 2011). The early-Holocene optimum was followed by a cold and dry period from 9.5–7.4 kyr BP, when low water levels occurred in lakes of the Larsemann Hills (Verleyen et al., 2004). Studies of marine sediments from Prydz Bay suggest warmer ocean conditions from 7.4–5.2 kyr BP (Verleyen et al., 2004). Penguin guano sediments from Gardner Island (68° 34′ S, 78° 52′ E), in the Vestfold Hills, also indicate a period of intense surface hydrodynamics between 7.0 and 6.7 kyr BP (Huang et al., 2009). In addition, a distinct mid-late Holocene thermal optimum was reconstructed in the Vestfold Hills. Pickard et al. (1986) proposed an optimum from 4.7–3.0 kyr BP based on a sediment record from Watts Lake (68° 35′ S, 78° 00′ E); and studies of lacustrine diatom assemblages indicated a warm and wet period from 4.2–2.2 kyr BP (Roberts and McMinn, 1996, 1999). Concurrent with many other locations in the East Antarctica, the Vestfold Hills experienced a neoglaciation at around 2.5 kyr BP (Ingólfsson, 2004; McMinn et al., 2001).

Despite the foregoing, the process of ice retreat during the last glacial-interglacial transition in the Vestfold Hills remains unclear (Mackintosh et al., 2014). Some parts of the Vestfold Hills may have been ice-free throughout the LGM (Last Glacial Maximum, Colhoun et al., 2010; Gibson et al., 2009); however, some lakes only became seasonally open at 11.4 kyr BP, when diatoms started to appear in the sediments (Roberts and McMinn, 1999; Cromer et al., 2005). Additional records come from adjacent areas. Offshore sediments from the central Rauer Islands (68° 51′ S, 77° 50′ E, Fig. 1) indicate that the ice-shelf receded from this location at around 13.3–12.7 kyr BP (Barbara et al., 2010). In addition, many lakes in the Larsemann Hills were fully

* Corresponding authors.
E-mail addresses: wangjianjun@tio.cn (J. Wang), zqxie@ustc.edu.cn (Z. Xie), slg@ustc.edu.cn (L. Sun).

https://doi.org/10.1016/j.palaeo.2017.11.053
Received 19 May 2017; Received in revised form 22 November 2017; Accepted 22 November 2017
Available online 28 November 2017
0031-0182/ © 2017 Published by Elsevier B.V.

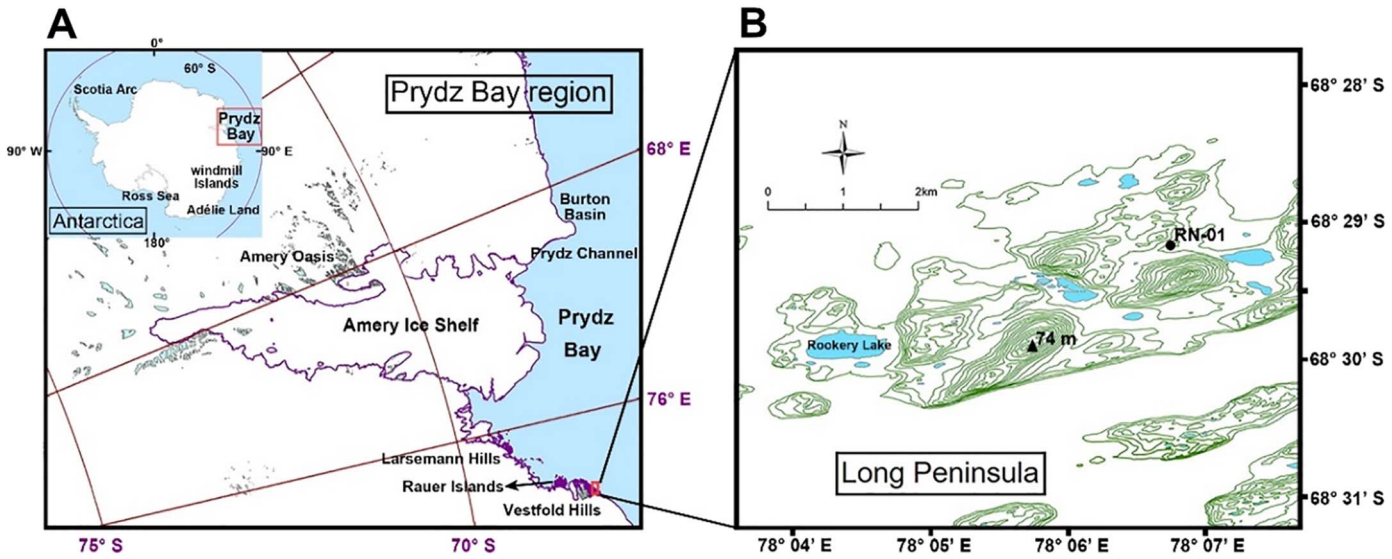

Fig. 1. The study area and sampling site of core RN-01 on Long Peninsula, Vestfold Hills, East Antarctica.
(A) Antarctica and the Prydz Bay region. (B) Long Peninsula. The sampling site of RN-01, on western Long Peninsula, is indicated by a filled circle. The contour interval is 5 m. Shape files are from SCAR, ADD at http://add.antarctica.ac.uk/repository/entry/show?entryid=f477219b-9121-44d6-afa6-d8552762dc45 for Antarctica and Prydz Bay, and from the Australian Antarctic Data Center at https://data.aad.gov.au/aadc/portal/drill_down.cfm?id=13 for the Vestfold Hills.

deglaciated from 14.5–11.5 kyr BP when organic sedimentation commenced (Hodgson et al., 2005; Verleyen et al., 2004, 2005). However, several lakes on Stoknes Peninsula (69° 26′ S, 76° 05′ E), in the Larsemann Hills, were not permanently ice-covered from, at the earliest, 40 kyr BP (Hodgson et al., 2001). Glacial deposits provide further evidence of the timing of the deglaciation. Deposition of glacial sediments in both Terrasovoje Lake and Beaver Lake at Amery Oasis (70° 40′ S, 68° 00′ E, Fig. 1) terminated at around 12.5–12.4 kyr BP (Wagner et al., 2004, 2007), and the areas below the current Amery ice shelf (69° 45′ S, 71° 00′ E) were transformed to an open water environment by 1.1 kyr BP (Barbara et al., 2010; Leventer et al., 2006; Mackintosh et al., 2014). The ice-shelf at Burton Basin (67° 35′ S, 68° 07′ E, Fig. 1), western Prydz Bay margin, was deglaciated at 12.8 kyr BP (Borchers et al., 2016), and a phase of glacial-marine deposition in the East Prydz Channel region (67° 30′ S, 72° 00′ E, Fig. 1) ended at around 13.0 kyr BP (Domack et al., 1998; Mackintosh et al., 2014).

East Antarctica currently has over 250 Adélie penguin (*Pygoscelis adeliae*) breeding sites and 30% of the global breeding pairs (Southwell et al., 2017; Lynch and LaRue, 2014). Studies of the modern ecology of Adélie penguins reveal a distinctive trend of population change in East Antarctic over a decadal scale, compared to some other parts of Antarctica. While the population of Adélie penguins in the Antarctic Peninsula has decreased over the last decades, the population in East Antarctica exhibits the opposite trend (Southwell et al., 2015).

However, the long-term history of Adélie penguin population dynamics in East Antarctica is less well known than in the Antarctic Peninsula and the Ross Sea region. Reconstructions of penguin populations for the early Holocene and earlier have only been performed by genetic researches. For example, Li et al. (2014) discerned a slight positive trend of the Adélie penguin population since 1 Myr BP; the trend became much significant at 150 kyr BP and then started to reverse following cooling at 60 kyr BP. However, these genetic reconstructions focused on the historical change of a specific lineage and they do not provide information on where the population change took place. The oldest fossil evidence of Adélie penguin colonization was a 45 kyr BP bone from the Ross Sea region (Emslie et al., 2007); however, no residuals were discovered dating to the LGM. During the last deglaciation, extensive ice-free grounds were produced, providing suitable breeding habitats for penguins, and, based on genetic studies, Adélie penguin populations in the Antarctic Peninsula began to expand from 16 kyr BP (Clucas et al., 2014). Younger et al. (2015) reconstructed changes in the population of Adélie penguins in East Antarctica from 20 kyr BP and noted an increase from ~14 kyr BP; this pattern corresponded to changes in the temperature record of the Dome C ice core and the timing of deglaciation recorded in many lakes in the Vestfold and Larsemann Hills (Cromer et al., 2005; Hodgson et al., 2001; Roberts and McMinn, 1999; Verleyen et al., 2004, 2005). However, this reconstruction has a large degree of temporal uncertainty, with a 95% confidence interval of 19–11 kyr BP (Younger et al., 2015); moreover, it does not provide information on the location of the reconstructed population.

Currently, the oldest geological evidence of East Antarctic penguin colonization is from 9 kyr BP and 8.5 kyr BP in records from the Windmill Islands (66° 20′ S, 110° 28′ E, Fig. 1, Emslie and Woehler, 2005) and Gardner Island, in the Vestfold Hills, respectively (Huang et al., 2009). However, these records commenced much later than the date of local ice retreat. Geological records of penguin colonization and habitat expansion following the last glacial-interglacial transition are generally absent in East Antarctica.

In the present study, we obtained a 15.6-kyr record from a sediment core (RN-01) from a small catchment on Long Peninsula, northern Vestfold Hills. Analyses of ^{14}C, lithology, grain size and geochemical proxies identified a phase of deglaciation characterized by rapid sediment accumulation and a high content of coarse-grained lithogenic material. Subsequently, we used multivariate statistical analysis of the geochemical proxies to estimate the time of initial penguin colonization and subsequent population changes over the last 14 kyr. We also compare our results with other reconstructions of seabird colonization processes in the Arctic and other areas of Antarctica, and discuss the primary drivers of penguin colony expansion following the last deglaciation.

2. Materials and methods

2.1. Study site and sample collection

Long Peninsula (68° 29′ S, 78° 07′ E) is in the northern Vestfold Hills, East Antarctica, about 20 km north of Davis Station. Long Peninsula is 7.41 km^2 in area, with the highest point at 74 m apsl (above present sea level, Harris et al., 2015, Fig. 1). The region on the

west coast of Long Peninsula is an important Adélie penguin summer habitat which comprises four separate breeding colonies (Southwell and Emmerson, 2013). According to a satellite census on December 2012 (Lynch and LaRue, 2014), approximately 45,497 pairs bred in the adjacent areas in summer. The predominant rock type of Long Peninsula is gneiss, and there is the scattered occurrence of norite, granulite and basalt dykes (Collerson et al., 1983; Harley, 1993).

The location of sediment core RN-01 is within a Mossel gneiss (Opx-Qz-Fd gneiss) zone (Collerson et al., 1983). The site is in a catchment in a depression on western Long Peninsula at an elevation of 10 m apsl. The catchment is on the back of a secondary terrace and is about 100 m northeast of an active Adélie sub-colony and 600 m southwest of the sea. The terrain around the catchment is covered by penguin guano, chick carcasses and residuals. The core was taken in January 2016 using a 6 cm (in diameter) PVC pipe and was sampled at 1-cm intervals to produce 59 samples.

2.2. Chronology

No macrofossils were recovered from RN-01, except in the uppermost sub-sample, and therefore 8 samples of bulk sediment were selected for AMS (Accelerator Mass Spectrometry) radiocarbon dating at the A.E. Lalonde AMS Laboratory, Ottawa University. Sample processing procedures are described in Crann et al. (2016). Calibration of ^{14}C ages and Bayesian age-depth modeling were done using the R package Calm v.2.2. Because penguins feed on marine-sourced organisms, the marine reservoir effect needs to be considered. The relative sea level of the Vestfold Hills, as reconstructed in previous research, was below 10 m apsl over the last 10 kyr (Hodgson et al., 2016), suggesting that core RN-01 was free of the direct input of marine-sourced materials during its interval of accumulation. Thus, the only potential source of aged marine organic carbon was penguin guano and remains. According to a consideration of the division of guano and non-guano phases (see Section 4.2), sub-samples from 34 to 59 cm were derived from terrestrial materials and were calibrated with the SHCal13 curve (Hogg et al., 2013). Sub-samples from above 34 cm were influenced by both penguin-derived and terrestrial sources and were calibrated with a curve which combined SHCal13 and Marine13 (Reimer et al., 2013). The fraction of the marine end was evaluated using the proportion of sea-bird sourced organic carbon of the total organic carbon (TOC) content. Assuming the organic matter input from non-penguin sources was constant throughout core RN-01, we defined the average TOC value of the interval from 34 to 59 cm as the non-marine background value. Therefore, the fraction of the marine end of the sub-sample for x-cm-depth is:

$$F_{marine,x} = (TOC_x - TOC_{34-59})/(TOC_x) \times 100\% \quad (1)$$

We used an averaged ΔR value of 779 ± 121, based on a series of paired U/Th and radiocarbon dates from trapped coral samples (Hall et al., 2010). This value is close to previously-published ΔR values, based on isolated pre-bomb radiocarbon dates (ΔR = 750 ± 50, Stuiver and Reimer, 1993; ΔR = 667 ± 55, Lambert et al., 2002; ΔR = 811 ± 102, Hofstee et al., 2006; ΔR = 779 ± 60, Stuiver et al., 1986).

2.3. Geochemical analysis

The ornithogenic sediment samples from core RN-01 were separated into sub-samples and then air-dried and ground to pass through a 74 μm mesh sieve. The sub-samples were then subjected to the following analyses.

Element contents of Cu, Zn, Co, Ni, P, Cr, K, Na, Ca, Mg, Fe, Al, Sr, Ba, Mn and Ti were measured by Atomic Emission Spectrometry. 0.245–0.255 g of each sub-sample was weighed and digested in Teflon tubes with a HNO_3-HCl-HF-$HClO_4$ digestion at 190 °C. Finally, the samples were dissolved in 10% HCl and analyzed by Inductively Coupled Plasma-Optical Emission Spectroscopy (ICP-OES, Perkin Elmer 2100DV).

Acid soluble Sr (ASSr) was measured by treating 0.245–0.255 g of sub-sample with 25 mL of 0.1 mol/L HCl followed by shaking for 8 h and centrifuging for 5 min at 3000 r/min. The supernatant was finally analyzed by ICP-OES.

Fluorine (F) was measured using the ion-selective-electron (ISE) method. 16 sub-samples weighing 0.245–0.255 g were mixed with 1 g of solid KOH and 3 g of solid NaOH in nickel crucibles. They were then fused at 650 °C in a muffle furnace and washed into glass beakers with 1:1 HCl and deionized water and acidified with 10 mL of HCl. The test solution was then diluted in two steps: 1) 10 mL of buffering agent (pH = 6.6) was added to the entire solution and then diluted into 100 mL with water; and 2) 10 mL of buffer agent was added to 10 mL of the solution obtained from step 1, adjusted to pH = 6.6, and diluted to 50 mL. A fluorion selective electrode and a calomel electrode were connected and inserted into the final solution and the electric potential difference was detected with a pXS-215 ion-activity meter. The fluorion concentration was calculated using a working curve constructed from F^- standard solutions of 0.5, 1, 2, 5, 10, and 20 ppm.

Total organic carbon (TOC) was measured by weighing 0.245–0.255 g of each sub-sample and adding precisely 10 mL of 0.8000 mol/L $K_2Cr_2O_7$ (equivalent electron concentration), and 5 mL of vitriol. The test solution was then heated in an oil bath for 5 min at 190 °C and air cooled; then, 10 mL of H_3PO_4 was added as a masking agent for Fe^{3+}, and titrated with 0.2 mol/L $(NH_4)_2Fe(SO_4)_2$. 0.2 mol/L sodium diphenylamine sulfonate was used as the titration indicator.

Cholesterol and cholestanol were analyzed by subjecting freeze-dried samples to Soxhlet extraction for 72 h with 9:1 dichloromethane/methanol. The extracts were concentrated by rotary evaporation and then saponified using 0.5 mol/L KOH/MeOH. Neutral lipids were partitioned out of the basic solution with hexane. Neutral lipids were further separated with 5% deactivated silica gel column chromatography using solvents of increasing polarity from hexane through methylene chloride. The fractions containing hydrocarbons (eluted with hexane) and n-alkanols/sterols (eluted with methylene chloride) were collected separately. The alcohol fraction was treated with BSTFA (*N*,*O*-bis-trimethylsilyltrifluoroacetamide) to form trimethylsilyl (TMS)-ether derivatives. The derivatives of the alcohol fraction (including n-alkanols and sterols derivates) were analyzed on a GCMS-QP2010 SE gas chromatograph-mass spectrometer with a DB5 (50 m × 0.32 mm × 0.25 m) capillary column (J&W). Helium was used as the carrier gas. The mass spectrometer was operated in EI mode at 70 eV. The GC oven was programmed as follows: hold 2 min at 60 °C, increase to 200 °C at 10 °C/min, increase to 280 °C at 3.5 °C/min, hold 15 min at 280 °C, increase to 300 °C at 1.5 °C/min, and hold 30 min at 300 °C. Analysis was performed in SCAN mode.

Grain-size analysis was conducted after removal of organic matter by weighing approximately 0.5 g of each unground sub-sample followed by treatment with 10 mL of 30% H_2O_2 at 150 °C until the reaction ceased. Test solutions were then decarbonated with 10 mL of 10% HCl and centrifuged for 5 min three times before adding 10 mL of 10% sodium hexametaphosphate as a dispersant. Grain-size distributions were measured using a Coulter LS 13320 laser grain size analyzer. Sorting coefficients were calculated using Eq. (2):

$$\text{Sorting coefficient} = (\varphi_{84} - \varphi_{16})/4 + (\varphi_{84} - \varphi_{16})/4 \quad (2)$$

where φ_p is the log base 2 value of the quantile of order p of sample diameters.

2.4. Data analysis

R-mode cluster analysis was carried out on scaled data of 21 geochemical proxies for the 59 sub-samples from core RN-01 using the "hclust" function and the "ward.D" parameter method of the R basic package (version 3.4.0). CONISS cluster analysis was performed on the square-root transformed geochemical data with the R package "rioja"

(Roberts et al., 2017). R-mode cluster analysis of the sub-samples older and younger 14.6 kyr BP (34-cm depth) was performed separately to investigate possible differences in proxy correlations for guano and non-guano phases. The cholestanol content was excluded from the cluster analysis because it was not detectable before 14.6 kyr BP.

Separate proxy-Fe cross-plots were produced for the geochemical data of three phases: 1) the guano phase (14.6 kyr BP to present); 2) 15.6–14.6 kyr BP; 3) the deglaciation phase (~15.6 kyr BP). Averaged element concentrations of bedrock and penguin guano were also plotted to illustrate sedimentary sources for the different phases. Penguin guano data were obtained from Gardner Island, in the Vestfold Hills (n = 3, Huang et al., 2011), and bedrock data were partly from Gardner Island (n = 3, Huang et al., 2011) and partly from the gneiss samples recovered from different depths throughout core RN-01 (n = 17).

Fe-normalized enrichment factors (EF) of the geochemical proxies were calculated with Eq. (3):

$$EF_i = (C_i/C_{Fe})_{sample}/(C_i/C_{Fe})_{background} \quad (3)$$

where EF_i and C_i are the enrichment factor and concentration of proxy i and C_{Fe} is the Fe concentration. According to the discussion in Section 4.1, the layer from 40 to 59 cm was formed during the deglaciation, at which time penguins were unlikely to have colonized the study location. We propose that the penguin-derived proxy levels at this stage represent the background values of non-penguin sources of a sedimentary component derived mainly from bedrock weathering. On this basis, we calculated the background C_i / C_{Fe} as the averaged values of the deglaciation phase of core RN-01 (~15.6 kyr BP, 40–59 cm).

Principal component analysis (PCA) was undertaken on scaled geochemical proxies using the "prcomp" function of the R basic package. Cholesterol and cholestanol were excluded because they were not detectable in several sub-samples. Finally, we used both the CONISS results and the trends of EF_P, EF_{ASSr}, EF_{TOC} and sample scores on –PC1 (the minus of the first principal component) to estimate the boundary between guano and non-guano phases. The value of the mean + SD (standard deviation) of the 40–59-cm interval was used as the cut-off for the guano phase.

3. Results

3.1. Chronology and lithology

An age-depth model for core RN-01 was established from the calibrated AMS ^{14}C dates listed in Table 1 (Fig. 2). The ages of the samples from 53 cm and 43 cm are reversed and there is a difference of about 200 yr, within the 95% confidence intervals (> 600 yr, Table 1). We propose that the interval from 53 to 43 cm was deposited near-instantaneously. Based on the characteristics of a relatively large median grain-size, grey-coloration of the sediments, and a large proportion of gravel (Fig. 2–3), we infer that this deposition phase probably spans the interval from 59 to 40 cm. In the Bayesian age-depth model, the interpolated age range of the interval from 59 to 40 cm is 15,797 to 15,400 yr BP (< 400 yr); consequently, we used the average value of the modeled ages for this interval (15,600 yr BP) as an age estimate (Fig. 2).

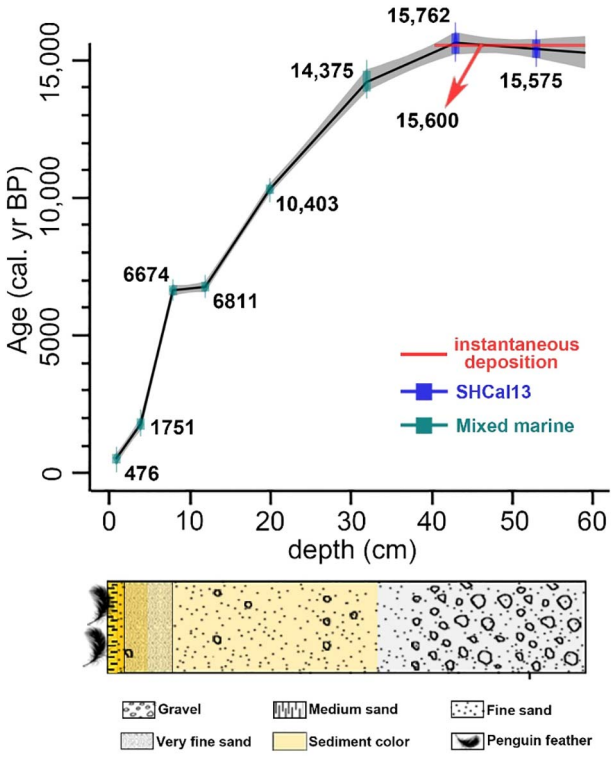

Fig. 2. Bayesian age-depth model and lithology of core RN-01.
Blue rectangles are dates calibrated as terrestrial-sourced materials and dark-green rectangles are dates calibrated as a mixture of terrestrial- and marine-sourced materials. The black line shows the best age estimates, the grey shading the 95% confidence intervals, and the red line the average age of the deglaciation phase. Calibrated age (yr BP) is shown by each data point. (For interpretation of the references to color in this figure legend, the reader is referred to the web version of this article.)

Table 1
Bulk sediment radiocarbon dating results for 8 sub-samples from core RN-01.

	Depth (cm)	Conventional ^{14}C age (yr BP)	Calibrated yr BP (95% confidence)	Calibration curve
RN-1	1	1515 ± 22	300–652	Mixed Marine SoHem*
RN-4	4	2621 ± 25	1546–1954	Mixed Marine SoHem*
RN-8	8	6434 ± 34	6494–6858	Mixed Marine SoHem*
RN-12	12	6525 ± 40	6637–6993	Mixed Marine SoHem*
RN-20	20	9575 ± 66	10,231–10,576	Mixed Marine SoHem*
RN-32	32	12,507 ± 80	13,998–14,767	Mixed Marine SoHem*
RN-43	43	13,210 ± 115	15,389–16,146	SHCal13
RN-53	53	13,054 ± 106	15,239–15,913	SHCal13

All the dated materials are bulk sediments.
* Mixed Marine SoHem: samples calibrated using a combination of SHCal13 and Marine13 (see Section 2.2).

For the remainder of core RN-01, the dates are in stratigraphic order and the age model appears reasonable. The depth interval from 40 to 12 cm spans the age range of 15,600–6811 yr BP, and the sediment accumulation rate (SAR) is relatively stable at ~314 yr / cm. The interval from 12 to 8 cm spans the age range 6811–6674 yr BP and thus the SAR was rapid (~31 yr / cm). The interval from 8 to 0 cm corresponds to the period from 6674 yr BP to present, with an average SAR of 835 yr / cm.

The median grain-size (Mz) of core RN-01 exhibits a three-stage decreasing trend from bottom to top, except for the two topmost samples (Fig. 3). Coarse grain sizes (78.1–130.8 μm) occur within the interval from 59 to 40 cm, corresponding to the rapidly-deposited grey gravel-dominated interval. The Mz from 39 to 9 cm range from 48.4–99.4 μm. The sediment color is grey from 39 to 34 cm and greyish-brown from 33 to 9 cm. From 8 to 3-cm depth, Mz ranges from 34.1–51.1 μm; the colors of this interval are greyish-brown from 8 to 6 cm and light-brown from 5 to 3 cm. The two topmost samples are dark-brown in color and penguin feathers were present on the core surface. From 59 to 15 cm the sorting coefficient (SC) fluctuates within a narrow range (2.00–2.43, average 2.22); there is a peak from 13 to 9 cm (maximum 2.60) and a trough from 8 to 3 cm. Overall, Mz and SC exhibit a similar pattern of variation.

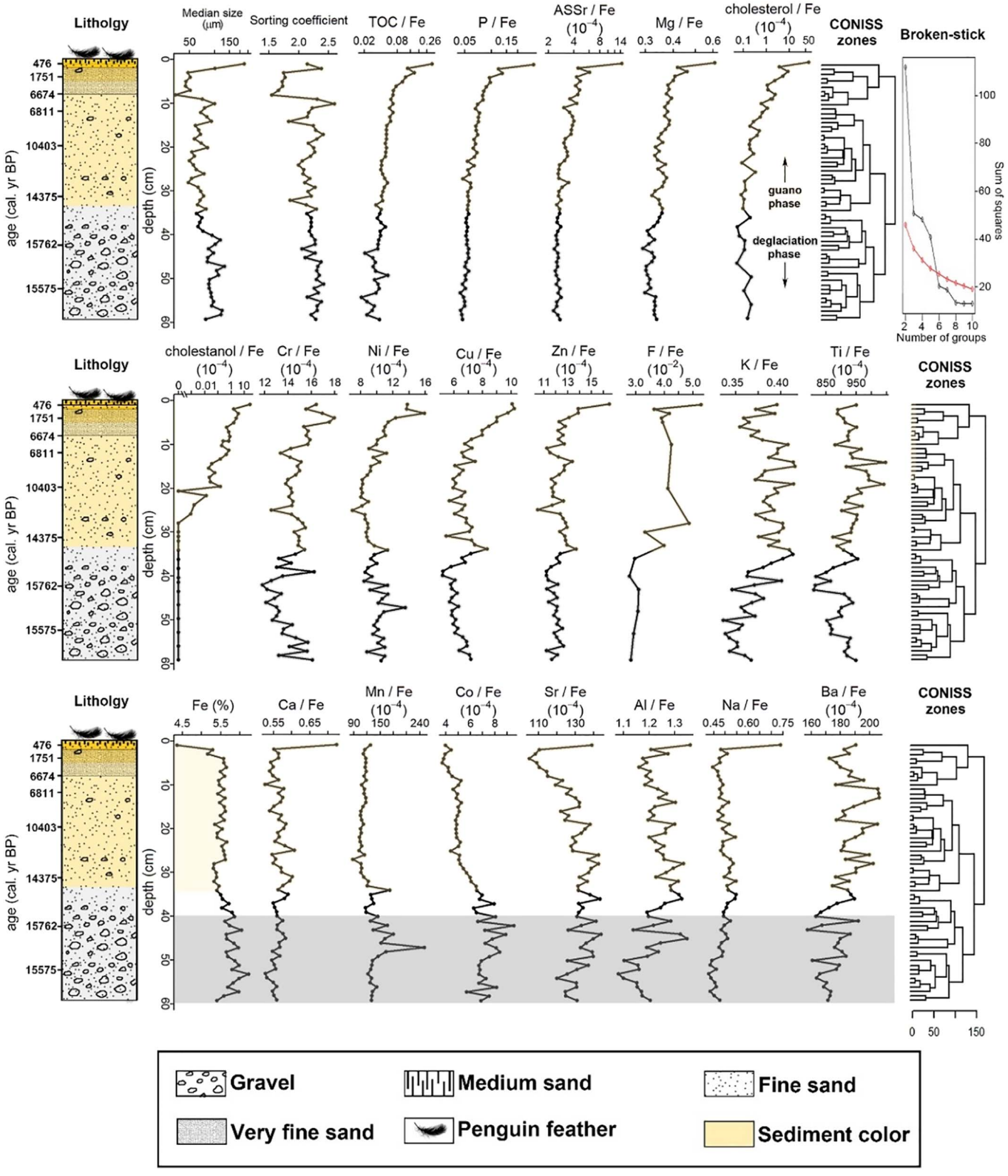

Fig. 3. Lithology, grain size, geochemical ratios and the results of cluster analysis (CONISS) of core RN-01.
The geochemical components are normalized to the Fe content. The grey and brown shaded zones show the deglaciation and guano phases, respectively. (For interpretation of the references to color in this figure legend, the reader is referred to the web version of this article.)

3.2. Geochemistry

Profiles of Fe-normalized geochemical proxies for core RN-01 are shown in Fig. 3 and cross-plots of selected proxies and the results of R-mode cluster analysis and PCA are shown in Fig. 4. The cross-plots show that sediments of core RN-01 are derived from the inputs of penguin-derived material and the products of bedrock weathering (Fig. 4A, Supplementary Table 1). The R-mode cluster analysis results separate

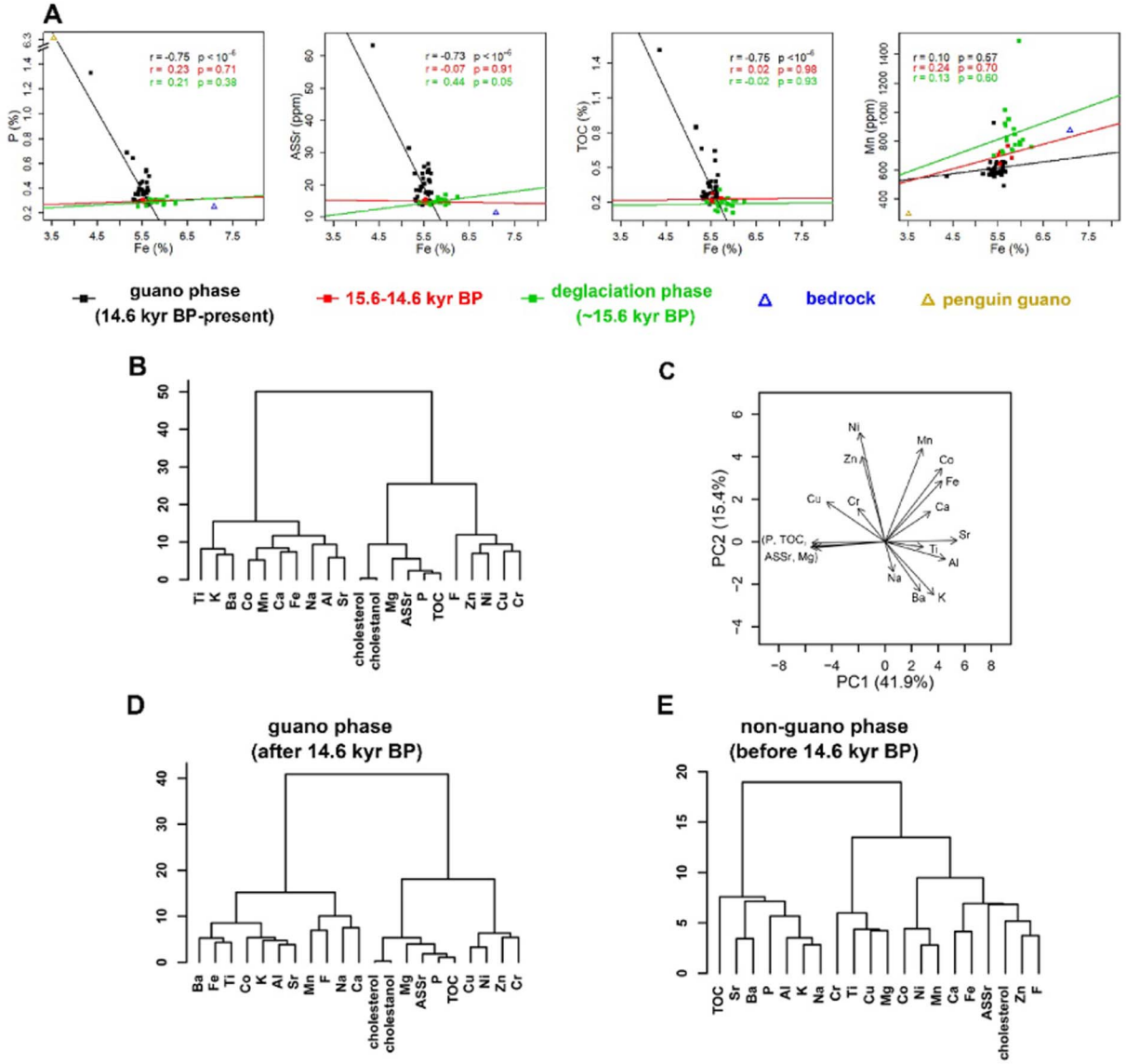

Fig. 4. Selected element-iron cross-plots, the results of R-mode cluster analysis and PCA of the geochemical data for core RN-01.
(A) Element-iron cross-plots for P, ASSr, TOC and Mn for three sediment age-groups 14.6 kyr BP-present – black squares; 15.6–14.6 kyr BP – red squares; and the deglaciation phase at 15.6 kyr BP – green squares. Lines of best fit for each group are also shown. The element composition of samples of bedrock and penguin guano is shown by blue and brown triangles, respectively. (B) Results of R-mode cluster analysis of 21 geochemical proxies for core RN-01. (C) PCA biplot showing the relationship between 18 proxies and the first two principal components for core RN-01. (D)–(E) Results of R-mode cluster analysis of the guano and non-guano datasets. (For interpretation of the references to color in this figure legend, the reader is referred to the web version of this article.)

the proxies into three groups (Fig. 4B, Supplementary Table 2): 1) penguin-derived (TOC, P, Mg, ASSr, cholesterol and cholestanol), 2) penguin-associated (Cr, Cu, Ni, Zn, F), and 3) lithogenic (Sr, Al, Na, Fe, Ca, Mn, Co, Ba, K, Ti).

The first cluster comprises P, TOC, ASSr, Mg, cholesterol and cholestanol (Fig. 4B), which are mainly from penguin-derived inputs to the sediment. These proxies exhibit an overall increasing trend from the bottom to the top of the core (Fig. 3). The levels are the lowest below ~34 cm, increase gradually above ~34 cm and rise rapidly from ~10 cm. The P content of the sediments is the most typical bioindicator for penguin inputs (Nie et al., 2015; Sun et al., 2000; Yang et al., 2018). P is transported from the ocean system, which is rich in P (Sands et al., 1998), to the terrestrial system by foraging penguins and enters the sediment along with guano and penguin remains. The P content in the local penguin guano far exceeds that of the bedrock (~25 times, Supplementary Table 1; Huang et al., 2011). Sr is also enriched in penguin feces and is considered a characteristic bio-element in some ornithogenic sediments in the Antarctic Peninsula (Sun et al., 2000; Roberts et al., 2017). In core RN-01, however, the total Sr content in penguin guano is at the same level as in the bedrock (Supplementary Table 1) and it exhibits a different trend from the penguin-derived and penguin-associated proxies. Isotope tracing revealed that the ASSr content of sediments is mainly derived from penguin inputs (Sun et al., 2005). In core RN-01, ASSr is lower than total Sr by one order of magnitude, and it corresponds with the trend of other penguin-derived proxies. TOC is apparently more enriched in penguin inputs than in material from bedrock erosion. The Mg content of local penguin guano is ~2.3 times higher than that in bedrock (Supplementary Table 1). The high correlation between P and Mg ($r = 0.83$, $p < 10^{-13}$, Supplementary Table 2) suggests the significant occurrence of struvite ($Mg(NH_4)PO_4{\cdot}6H_2O$), a typical component of ornithogenic soils and sediments (Tatur and Keck, 1990). Mg was also a penguin-indicating element in an ornithogenic core from Zolotov Island, in the Vestfold Hills (Huang et al., 2011). Cholesterol and cholestanol are organic

bioindicators and are absent in bedrock; thus, they have been used to represent penguin fecal influence in ornithogenic sediments (Wang et al., 2007).

The second cluster comprises Cr, Cu, Ni, Zn and F and is located close to the penguin-derived cluster (Fig. 4B); it is associated with both penguin inputs and the input of material from bedrock weathering. Cu, Zn and F are typical penguin-indicating elements in the Antarctic Peninsula, Ross Sea region and East Antarctica (Nie et al., 2015; Sun et al., 2000; Huang et al., 2009; Roberts et al., 2017). In the region, the Cu content in penguin guano is about 7.5 times higher than that in bedrock, and the Zn content is 1.4 times higher in guano than in bedrock. In core RN-01, Cu and Zn are associated with guano input but are also influenced by bedrock erosion. F is highly enriched in krill (Soevik and Braekkan, 1979), which is a major food for penguins (Huang et al., 2013). The Ni content in local guano is 1.9 times lower than that of bedrock; however, Ni tends to be enriched in organic matter and in the sediment fine fraction during sedimentation processes (Lewan and Maynard, 1982), and thus is strongly correlated with other penguin-associated proxies (Supplementary Table 2). Cr was not detected in the penguin guano of the Vestfold Hills (Supplementary Table 2); however, Cr is known to be adsorbed to and precipitated with struvite by several mechanisms (Rouff, 2012). In core RN-01, Cr, Cu, Zn, and Ni exhibit a greater amplitude of variability and an increasing trend above ~10 cm (Fig. 3). The F content of the sediments above ~33 cm (average of 2193 ± 219 ppm, $n = 10$) is significantly higher than that below (average of at 1706 ± 130 ppm, $n = 6$) (Fig. 3).

The third cluster includes Sr, Al, Na, Fe, Ca, Mn, Co, Ba, K, and Ti, which are typical lithogenic elements and they show minor fluctuations in the down-core plots (Fig. 3). The contents of these proxies are either higher in the bedrock than in penguin guano, or at the same level in the two end members (Supplementary Table 1).

4. Discussion

4.1. Identification of the deglaciation stage

According to the chronology, lithology and grain-size data for core RN-01 (Table 1, Fig. 2–3), the layer between 59 and 40 cm was deposited near-instantaneously at ~15.6 kyr BP (Section 3.1). The layer is highly inorganic with the lowest TOC content (< 0.2%) and the coarsest grain size (Fig. 3). In element-iron cross-plots, the geochemical composition of the sediments between 59 and 40 cm is close to that of the lithogenic background, indicating the dominant contribution of weathered materials (Fig. 4A). This layer could possibly be derived from sea water intrusion caused by storm surges or a rising sea level (Nie et al., 2015); however, this is unlikely since the relative sea level at that time was far lower than the sampling site (Hodgson et al., 2016). More likely, the layer was formed by the abrupt deposition of coarse-grained inorganic material associated with the deglaciation process (Leonard, 1997; Verleyen et al., 2004). This may have occurred in two ways: First, when the ice sheet covering the sampling site receded in response to climatic warming, terrigenous materials carried by the ice were released within a short time interval. These materials had large grain-sizes because of the strong transport capacity of the ice. Second, intensive meltwater flux, and thus enhanced surface hydrodynamic conditions, resulted in the rapid deposition of coarse-grained sediments. The very low TOC content of this layer is unsurprising: by the time of deglaciation, terrestrial primary productivity and the terrestrial biomass were very low. Thus, we infer that the layer between 59 and 40 cm represents the rapid deposition of coarse-grained sediments resulting directly from glacier retreat, at ~15.6 kyr BP. Subsequently, the deposition rate returned to a normal level and the median grain-size decreased, corresponding to the end of deglaciation.

Additional evidence for the timing of deglaciation is from nearby Ace Lake and Abraxas Lake on Long Peninsula. Study of diatom assemblages indicates that Ace Lake became an open water system at 13.4–13.2 kyr BP (calibrated age of 11.4 kyr BP, Roberts and McMinn, 1999). In addition, Abraxas Lake was likely without permanent ice cover in the last 23–21 kyr BP or longer (Gibson et al., 2009). The northeastern Vestfold Hills, which are closer to the present ice cap, was completely deglaciated at 11 kyr BP (Fabel et al., 1997). East Antarctic ice cores record a relatively warm interval from 15 to 14 kyr BP before the ACR (Antarctic Cold Reversal, Stenni et al., 2011), which was a possible cause of the 15.6 kyr BP deglaciation.

4.2. Identification of the guano phase and the date of initial penguin colonization

CONISS cluster analysis of the geochemical data separates the samples of core RN-01 into five zones (Fig. 3, Supplementary Table 3). Zone 3–5 (0–34 cm, 14.6 kyr BP-present) is characterized by enhanced levels of the penguin-derived proxies and by greyish-brown to dark-brown sediments and is identified as the guano phase. Zone 1–2 (34–59 cm, 14.6–15.6 kyr BP) is characterized by consistently low levels of the penguin-derived proxies and by grey-colored sediments, and is identified as the non-guano phase. The Fe-normalized EFs of the penguin-derived proxies represent the net contribution of penguin inputs to the sediment without the background influence (Fig. 5). Similarly, the minus first principal component (–PC1) loadings of core RN-01 mainly reflects changes in penguin-derived proxies and is interpreted as a measure of penguin inputs to the sediment (Fig. 4C, Supplementary Table 4). The boundary between the guano and non-guano phases as inferred from the trends in EF (EF_P, EF_{ASSr}, EF_{TOC}) values and sample scores on the –PC1 axis is from 14.4 to 14.8 kyr BP, with an average of 14.6 kyr BP (Fig. 5, Method 2.4), which agrees well with the results obtained from the CONISS cluster analysis.

Element-iron cross-plots indicate that the geochemical compositions of the deglaciation phase (~15.6 kyr BP) and for the interval from 15.6–14.6 kyr BP are similar to each other and to the bedrock (Fig. 4A); while the composition of the interval from 14.6 kyr BP-present is close to that of penguin guano. Moreover, the R-mode cluster analysis results and correlation coefficients for the intervals before and after 14.6 kyr BP reveal different relationships between the elements (Fig. 4D–E, Supplementary Table 5–6). The younger interval has stronger inverse correlations between biological and lithogenic proxies and forms more distant clusters (Supplementary Table 5). In addition, the cluster analysis results for the younger interval are very similar to those of the whole of core RN-01 (Fig. 4B and D). For the older interval, the inverse correlations between biological and lithogenic elements are less significant and the cluster analysis does not separate the penguin-derived or penguin-associated proxies from the lithogenic proxies (Supplementary Table 6, Fig. 4E). This evidence further supports a major shift in the sedimentary environment or sediment sources of core RN-01 at ~14.6 kyr BP. Therefore, we propose to use 14.6 yr BP as the initiation time of the guano phase.

Variations of the bioindicators in core RN-01 represent the evolution of the sampling site as a penguin breeding colony. The signals of the penguin-derived proxies represent the relative proportion of biological inputs from penguins. The sampling site of core RN-01 is a water catchment in a low-lying depression. At the time of sampling, the site was surrounded by active and abandoned sub-colonies, indicated by brown-colored ornithogenic soils, guano and penguin remains. The sediments of core RN-01 were sourced from water-transported weathering products and penguin droppings that were supplied to the ground surface by one or several sub-colonies surrounding the catchment. When the population increased within these sub-colonies, more droppings were produced and incorporated into the sediments, leading to an increased proportion of the penguin-derived proxies. The change in this population can be measured by the sample scores on –PC1. The shift from the non-guano to the guano phase represents the initial penguin colonization and the subsequent variations in sample scores on –PC1 reflect local population changes thereafter (Fig. 6).

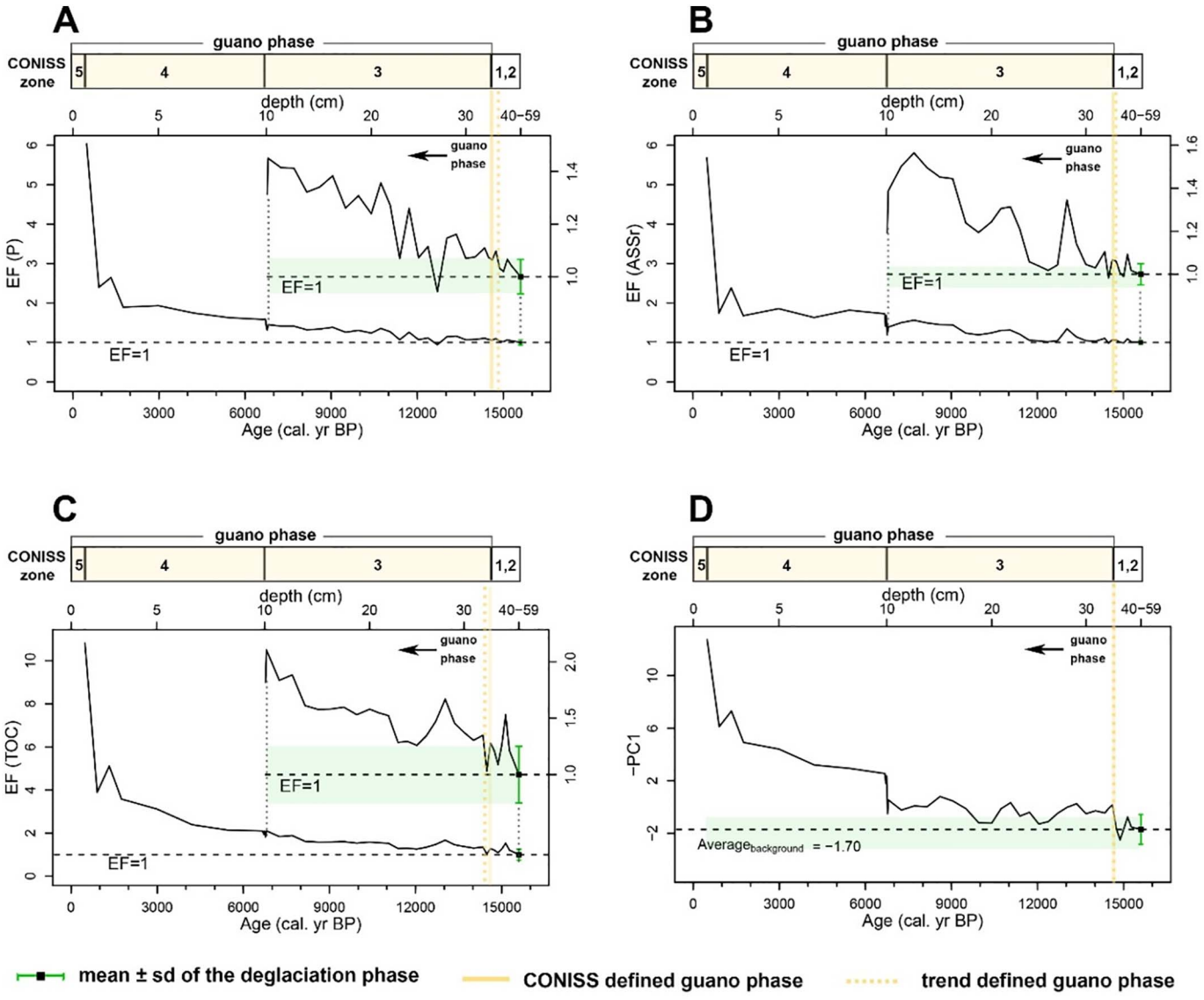

Fig. 5. Selected Fe-normalized enrichment factors and sample scores on –PC1 of core RN-01.
(A)–(C) Fe-normalized enrichment factors of P, ASSr and TOC. Data between 15.6 and 6.8 kyr BP (11–59 cm) are also shown plotted on expanded scales to show detailed variations. (D) Sample scores on –PC1 for core RN-01. Green bars and rectangles give the range of the mean ± SD of the background levels of EFs and –PC1 as inferred from the deglaciation phase. CONISS zones are drawn above the plots. Brown solid and dotted lines show the guano phase defined by the CONISS cluster analysis and the trend of EFs and –PC1, respectively. (For interpretation of the references to color in this figure legend, the reader is referred to the web version of this article.)

The initiation of the nearby penguin sub-colonies occurred at ~14.6 kyr BP, about 1.0 kyr after local deglaciation. This observation is the earliest geological record of penguin colonization in East Antarctica and agrees with a regional reconstruction based on previous genetic studies of the Adélie penguin history of East Antarctica, which revealed continuous population growth since ~14 kyr BP, with an eventual 135-fold expansion (Fig. 6, Younger et al., 2015). Two major refugia of Adélie penguins were reported during the LGM. One is located near the Ross Sea, and the second within Scotia Arc, Ross Sea region and East Antarctica (Li et al., 2014; Ritchie et al., 2004; Younger et al., 2015). The second lineage is presently comprised of individuals from all three regions, including East Antarctica (Younger et al., 2015). The colonization initiation time of 14.6 kyr BP, as inferred from core RN-01, is close to that of the East Antarctic Adélie penguin population growth reported by Younger et al. (2015). Furthermore, the deglaciation in other parts of East Antarctica was no earlier than 14 kyr BP (Verleyen et al., 2011). Therefore, the ancient colony of the Vestfold Hills at our study site was either part of the East Antarctic refuge, or was one of the earliest Adélie penguin breeding colonies in East Antarctica.

Suitable areas of ice-free grounds, food availability and sea ice conditions are key factors for Adélie penguin populations and colony growth on different time-scales (Younger et al., 2015). The first factor is thought to be the primary controller of the colonization process during glacial-interglacial transitions in many parts of Antarctica. In the Antarctic Peninsula, genetic studies reconstructed population growth from 16 kyr BP (Clucas et al., 2014), roughly concurrent with regional deglaciation (Hodgson et al., 2014; O Cofaigh et al., 2014). The oldest sedimentary record of Gentoo penguin occupation from the South Shetland Islands was 6.7 kyr BP (Roberts et al., 2017), 2000 years after the end of local deglaciation (Milliken et al., 2009), and this time lag was possibly due to eruptive volcanic activity. In the Ross Sea region, the earliest record of penguin presence was from Terra Nova Bay, 8 kyr BP (Baroni and Orombelli, 1994; Lambert et al., 2002), the time when the Ross Glacier retreated from the area (Baroni and Hall, 2004). In the past 45 kyr, colony abandonment and reoccupation of Adélie penguins in the Ross Sea region has been shown to follow the historical dynamics of the Ross Ice Sheet (Emslie et al., 2007). In the Windmill Islands,

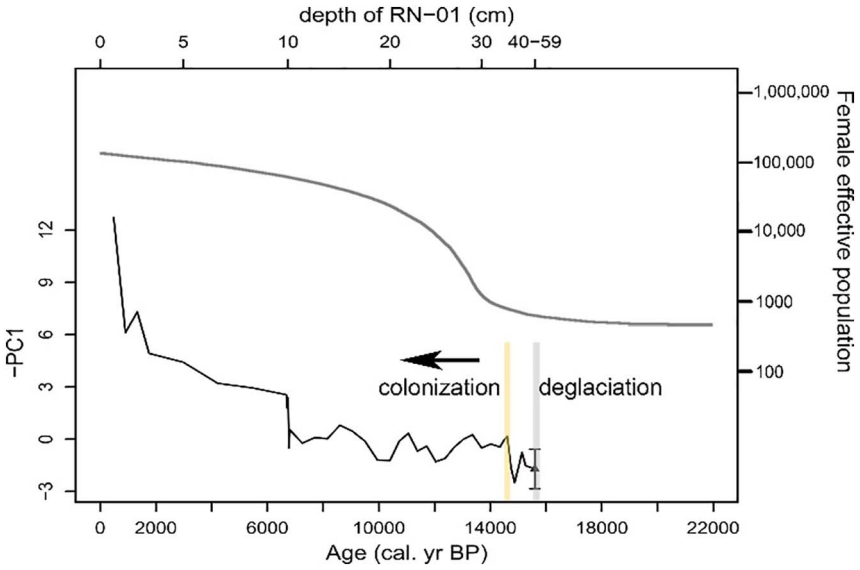

Fig. 6. Reconstructed local and regional penguin population change during the last ~20 kyr.
Local population change at the study site on Long Peninsula, northern Vestfold Hills, is measured by sample scores on the –PC1 axis for core RN-01 and is compared with the regional female effective population reconstructed by Younger et al. (2015). Grey and brown solid lines indicate the local deglaciation time and the local initiation of penguin colonization. (For interpretation of the references to color in this figure legend, the reader is referred to the web version of this article.)

East Antarctica, Adélie penguins colonized the islands no later than 9 kyr BP (Emslie and Woehler, 2005), while a local off-shore marine sediment record revealed the ice sheet retreated at 10.7–9.7 kyr BP (Hodgson et al., 2003). In the Arctic, seabirds inhabited Ny-Ålesund since 9.4 kyr BP, immediately after the complete deglaciation of Kongsfjorden at 9440 ± 130 yr BP (Yuan et al., 2010).

The increase in primary productivity during the early Holocene generally lagged deglaciation. A marine sediment record from off Adélie Land (75° 00′ S, 139° 00′ E) indicated that East Antarctic oceanic productivity was consistently low until 7.5 kyr BP in the mid-Holocene (Denis et al., 2009). The occupation time of Adélie penguins reported in the present study and in previous records from the Vestfold Hills and Windmill Islands (Emslie and Woehler, 2005; Huang et al., 2009) is much earlier than 7.5 kyr BP. Early Holocene productivity in the Antarctic Peninsula and Ross Sea region began to increase from ~9 kyr BP (Taylor et al., 2001) and 7.1 kyr BP (Younger et al., 2016), respectively; in both cases, this is later than regional ice retreat and penguin colonization.

Circumpolar Antarctic marine sediment reconstructions showed that the winter sea ice during the LGM was twice as extensive as today, but the summer sea ice was close (Gersonde et al., 2005). Historical sea-ice reconstructions are unable to distinguish between fast-ice and pack-ice (Younger et al., 2015), which have different impacts on Adélie penguins. Pack-ice has two opposing effects. On the one hand, pack-ice zones are primary summer fishing and wintering grounds (Ainley et al., 2010), and insufficient pack-ice could reduce krill abundance (Nicol et al., 2000; Wilson et al., 2001). On the other hand, pack-ice enhances water stratification and weakens vertical upwelling, leading to a low level of nutrients in the euphotic zone (Denis et al., 2010). Fast-ice prolongs the foraging distance of adult penguins and thus the provision intervals, leading to emaciated chicks and low breeding success (Cottin et al., 2012; Emmerson and Southwell, 2008; Ropert-Coudert et al., 2015). Although total summer sea- ice extent during the LGM was close to the present-day level, it is unclear whether the ratio of fast-ice and pack-ice was the same at both times. However, it is possible to speculate that during the last glacial-interglacial transition, weakened katabatic winds occurred which favored near-shore fast-ice formation (Adolphs and Wendler, 1995; Sprenk et al., 2014; Weber et al., 2011). Post-glacial sea ice conditions were probably not more favorable for Adélie penguins than that of glacial times. Thus, sea ice conditions were unlikely to be the main driver of Adélie penguin population growth after deglaciation.

4.3. Local penguin population change after initial colonization

After 14.6 kyr BP, all the penguin-derived proxies and –PC1 sample scores exhibit an overall positive trend (Figs. 3, 5, 6). From 14.6 to 6.8 yr BP, the increase is slight and the penguin population was probably very small during this stage. At ~6.8 kyr BP, the population started to increase rapidly, coincident with a second phase of rapid sediment deposition (of 4 cm or more) at around 6.8–6.7 kyr BP. This phase is characterized by a coarse sediment grain-size and large SC values. A similar pattern of deposition with an abnormally sediment accumulation rate is evident in contemporaneous records (7.0–6.7 kyr BP) from Gardner Island, in the Vestfold Hills, implying increased overland runoff and a humid climate (Huang et al., 2009). Although there were several climatic cooling phases at Amery Oasis (Cremer et al., 2007), Rauer Islands (Berg et al., 2010), Bunger Hills (Kulbe et al., 2001) and Windmill Islands (Emslie and Woehler, 2005), local evidence from Anderson Lake, in the southern Vestfold Hills, suggests high productivity and warmer conditions from 7.0–6.0 kyr BP (Roberts and McMinn, 1998). A climatic optimum with open-water conditions in spring and summer from 7.4–5.2 kyr BP was also revealed by a record of siliceous microfossils from lake sediments of the Larsemann Hills (Verleyen et al., 2004). A local warm and wet episode in the Vestfold Hills at 6.8–6.7 kyr BP likely provided favorable conditions for penguin reproduction. According to the –PC1 signal, the population of the sub-colonies around the site of core RN-01 increased over the last 6 kyr. Unfortunately, however, the low temporal resolution of the sub-surface layers makes it difficult to infer recent variations in the population size of these sub-colonies.

Although this study is the oldest record of penguin occupation of East Antarctica, our data are insufficient for examining the population history of Adélie penguins on a regional scale. Larger-scale and multi-proxy investigations are needed to provide further information on the location of glacial refugia during the LGM, and the timing and trajectory of the interglacial expansion.

5. Conclusions

Study of an ornithogenic sediment core from western Long Peninsula, in the Vestfold Hills, East Antarctica, revealed a 19-cm-thick near-instantaneously deposited layer and dates the local deglaciation time to ~15.6 kyr BP, 2000 years earlier than most of the other records from the region. Penguins started to colonize the area at ~14.6 kyr BP, 6000 years earlier than previous records from the Vestfold Hills. Moreover, the sampling site was likely the location of one of the earliest

Adélie penguin breeding colonies in East Antarctica. Furthermore, we propose that population growth and colony expansion during the last glacial-interglacial transition were mainly driven by the availability of extensive summer ice-free grounds generated from ice retreat.

Supplementary data to this article can be found online at https://doi.org/10.1016/j.palaeo.2017.11.053.

Acknowledgments

This study was funded by the Chinese Polar Environment Comprehensive Investigation & Assessment Programs (Grant CHINARE2016-02-01-03), the International Cooperation in Polar Research (Grant IC201604) and the NSF (Grant 417723). It was also supported by the Australian Antarctic program via Australian Antarctic Science Projects #4087 and #4088. All field procedures were approved by the Australian Antarctic Animal Ethics Committee (AAAEC). Sample information and data were provided by the Resource Sharing Platform of Polar Samples (http://birds.chinare.org.cn) and was maintained by Polar Research Institute of China (PRIC) and Chinese National Arctic & Antarctic Data Center (CN-NADC).

References

Adolphs, U., Wendler, G., 1995. A pilot-study on the interactions between katabatic winds and polynyas at the Adelie coast, eastern Antarctica. Antarct. Sci. 7, 307–314.
Ainley, D., Russell, J., Jenouvrier, S., Woehler, E., Lyver, P.O.B., Fraser, W.R., Kooyman, G.L., 2010. Antarctic penguin response to habitat change as Earth's troposphere reaches 2 degrees C above preindustrial levels. Ecol. Monogr. 80, 49–66.
Barbara, L., Crosta, X., Masse, G., Ther, O., 2010. Deglacial environments in eastern Prydz Bay, East Antarctica. Quat. Sci. Rev. 29, 2731–2740.
Baroni, C., Hall, B.L., 2004. A new Holocene relative sea-level curve for Terra Nova Bay, Victoria Land, Antarctica. J. Quat. Sci. 19, 377–396.
Baroni, C., Orombelli, G., 1994. Abandoned penguin rookeries as Holocene paleoclimatic indicators in Antarctica. Geology 22, 23–26.
Berg, S., Wagner, B., Cremer, H., Leng, M.J., Melles, M., 2010. Late Quaternary environmental and climate history of Rauer Group, East Antarctica. Palaeogeogr. Palaeoclimatol. Palaeoecol. 297, 201–213.
Borchers, A., Dietze, E., Kuhn, G., Esper, O., Voigt, I., Hartmann, K., Diekmann, B., 2016. Holocene ice dynamics and bottom-water formation associated with Cape Darnley polynya activity recorded in Burton Basin, East Antarctica. Mar. Geophys. Res. 37, 49–70.
Clucas, G.V., Dunn, M.J., Dyke, G., Emslie, S.D., Levy, H., Naveen, R., Polito, M.J., Pybus, O.G., Rogers, A.D., Hart, T., 2014. A reversal of fortunes: climate change 'winners' and 'losers' in Antarctic Peninsula penguins. Sci. Rep. 4.
Cofaigh, O., Davies, B.J., Livingstone, S.J., Smith, J.A., Johnson, J.S., Hocking, E.P., Hodgson, D.A., Anderson, J.B., Bentley, M.J., Canals, M., Domack, E., Dowdeswell, J.A., Evans, J., Glasser, N.F., Hillenbrand, C.D., Larter, R.D., Roberts, S.J., Simms, A.R., 2014. Reconstruction of ice-sheet changes in the Antarctic Peninsula since the Last Glacial Maximum. Quat. Sci. Rev. 100, 87–110.
Colhoun, E.A., Kiernan, K.W., McConnell, A., Quilty, P.G., Fink, D., Murray-Wallace, C.V., Whitehead, J., 2010. Late Pliocene age of glacial deposits at Heidemann Valley, East Antarctica: evidence for the last major glaciation in the Vestfold Hills. Antarct. Sci. 22, 53–64.
Collerson, K., Sheraton, J., Arriens, P., 1983. Granulite Facies Metamorphic Conditions During the Archaean Evolution and Late Proterozoic Reworking of the Vestfold Block, Eastern Antarctica. Lithosphere Dynamics and Evolution of Continental Crust (Abstract). Geol Soc Aust, Canberra, pp. 53–54.
Cottin, M., Raymond, B., Kato, A., Amelineau, F., Le Maho, Y., Raclot, T., Galton-Fenzi, B., Meijers, A., Ropert-Coudert, Y., 2012. Foraging strategies of male Adelie penguins during their first incubation trip in relation to environmental conditions. Mar. Biol. 159, 1843–1852.
Crann, C.A., Murseli, S., St-Jean, G., Zhao, X., Clark, I.D., Kieser, W.E., 2016. First status report on radiocarbon sample preparation techniques at the AE Lalonde AMS Laboratory (Ottawa, Canada). Radiocarbon 1–10.
Cremer, H., Heiri, O., Wagner, B., Wagner-Cremer, F., 2007. Abrupt climate warming in East Antarctica during the early Holocene. Quat. Sci. Rev. 26, 2012–2018.
Cromer, L., Gibson, J.A.E., Swadling, K.M., Ritz, D.A., 2005. Faunal microfossils: indicators of Holocene ecological change in a saline Antarctic lake. Palaeogeogr. Palaeoclimatol. Palaeoecol. 221, 83–97.
Denis, D., Crosta, X., Schmidt, S., Carson, D.S., Ganeshram, R.S., Renssen, H., Crespin, J., Ther, O., Billy, I., Giraudeau, J., 2009. Holocene productivity changes off Adélie Land (East Antarctica). Paleoceanography 24.
Denis, D., Crosta, X., Barbara, L., Masse, G., Renssen, H., Ther, O., Giraudeau, J., 2010. Sea ice and wind variability during the Holocene in East Antarctica: insight on middle-high latitude coupling. Quat. Sci. Rev. 29, 3709–3719.
Domack, E., O'Brien, P., Harris, P., Taylor, F., Quilty, P.G., De Santis, L., Raker, B., 1998. Late Quaternary sediment facies in Prydz Bay, East Antarctica and their relationship to glacial advance onto the continental shelf. Antarct. Sci. 10, 236–246.
Emmerson, L., Southwell, C., 2008. Sea ice cover and its influence on Adelie Penguin reproductive performance. Ecology 89, 2096–2102.
Emslie, S.D., Woehler, E.J., 2005. A 9000-year record of Adelie penguin occupation and diet in the Windmill Islands, East Antarctica. Antarct. Sci. 17, 57–66.
Emslie, S.D., Coats, L., Licht, K., 2007. A 45,000yr record of Adelie penguins and climate change in the Ross Sea, Antarctica. Geology 35, 61–64.
Fabel, D., Stone, J., Fifield, L., Cresswell, R., 1997. Deglaciation of the Vestfold Hills, East Antarctica: preliminary evidence from exposure dating of three subglacial erratics. In: RICCI, CA, The Antarctic Region: Geological Evolution and Processes. Terra Antartica Publications, Siena, pp. 829–834.
Gersonde, R., Crosta, X., Abelmann, A., Armand, L., 2005. Sea-surface temperature and sea ice distribution of the Southern Ocean at the EPILOG Last Glacial Maximum - a circum-Antarctic view based on siliceous microfossil records. Quat. Sci. Rev. 24, 869–896.
Gibson, J.A.E., Paterson, K.S., White, C.A., Swadling, K.M., 2009. Evidence for the continued existence of Abraxas Lake, Vestfold Hills, East Antarctica during the Last Glacial Maximum. Antarct. Sci. 21, 269–278.
Hall, B.L., Henderson, G.M., Baroni, C., Kellogg, T.B., 2010. Constant Holocene Southern-Ocean C-14 reservoir ages and ice-shelf flow rates. Earth Planet. Sci. Lett. 296, 115–123.
Harley, S.L., 1993. Sapphirine granulites from the Vestfold hills, east Antarctica - geochemical and metamorphic evolution. Antarct. Sci. 5, 389–402.
Harris, C., Lorenz, K., van Franeker, J., 2015. Important Bird Areas in Antarctica 2015. BirdLife Int. and Env. Research & Assessment.
Hodgson, D.A., Noon, P.E., Vyverman, W., Bryant, C.L., Gore, D.B., Appleby, P., Gilmour, M., Verleyen, E., Sabbe, K., Jones, V.J., Ellis-Evans, J.C., Wood, P.B., 2001. Were the Larsemann Hills ice-free through the Last Glacial Maximum? Antarct. Sci. 13, 440–454.
Hodgson, D.A., McMinn, A., Kirkup, H., Cremer, H., Gore, D., Melles, M., Roberts, D., Montiel, P., 2003. Colonization, succession, and extinction of marine floras during a glacial cycle: a case study from the Windmill Islands (east Antarctica) using biomarkers. Paleoceanography 18.
Hodgson, D.A., Verleyen, E., Sabbe, K., Squier, A.H., Keely, B.J., Leng, M.J., Saunders, K.M., Vyverman, W., 2005. Late Quaternary climate-driven environmental change in the Larsemann Hills, East Antarctica, multi-proxy evidence from a lake sediment core. Quat. Res. 64, 83–99.
Hodgson, D.A., Graham, A.G.C., Roberts, S.J., Bentley, M.J., Cofaigh, C.O., Verleyen, E., Vyverman, W., Jomelli, V., Favier, V., Brunstein, D., Verfaillie, D., Colhoun, E.A., Saunders, K.M., Selkirk, P.M., Mackintosh, A., Hedding, D.W., Nel, W., Hall, K., McGlone, M.S., Van der Putten, N., Dickens, W.A., Smith, J.A., 2014. Terrestrial and submarine evidence for the extent and timing of the Last Glacial Maximum and the onset of deglaciation on the maritime-Antarctic and sub-Antarctic islands. Quat. Sci. Rev. 100, 137–158.
Hodgson, D.A., Whitehouse, P.L., De Cort, G., Berg, S., Verleyen, E., Tavernier, I., Roberts, S.J., Vyverman, W., Sabbe, K., O'Brien, P., 2016. Rapid early Holocene sea-level rise in Prydz Bay, East Antarctica. Glob. Planet. Chang. 139, 128–140.
Hofstee, E.H., Balks, M.R., Petchey, F., Campbell, D.I., 2006. Soils of Seabee hook, cape Hallett, northern Victoria Land, Antarctica. Antarct. Sci. 18, 473–486.
Hogg, A.G., Hua, Q., Blackwell, P.G., Niu, M., Buck, C.E., Guilderson, T.P., Heaton, T.J., Palmer, J.G., Reimer, P.J., Reimer, R.W., Turney, C.S.M., Zimmerman, S.R.H., 2013. Shcal13 southern hemisphere calibration, 0–50,000 years Cal Bp. Radiocarbon 55, 1889–1903.
Huang, T., Sun, L., Wang, Y., Liu, X., Zhu, R., 2009. Penguin population dynamics for the past 8500 years at Gardner Island, Vestfold Hills. Antarct. Sci. 21, 571–578.
Huang, T., Sun, L., Wang, Y., Kong, D., 2011. Late Holocene Ad, lie penguin population dynamics at Zolotov Island, Vestfold Hills, Antarctica. J. Paleolimnol. 45, 273–285.
Huang, T., Sun, L., Long, N., Wang, Y., Huang, W., 2013. Penguin tissue as a proxy for relative krill abundance in East Antarctica during the Holocene. Sci. Rep. 3.
Ingólfsson, Ó., 2004. Quaternary glacial and climate history of Antarctica. Dev. Quaternary Sci. 2, 3–43.
Kulbe, T., Melles, M., Verkulich, S.R., Pushina, Z.V., 2001. East Antarctic climate and environmental variability over the last 9400 years inferred from marine sediments of the Bunger Oasis. Arct. Antarct. Alp. Res. 33, 223–230.
Lambert, D.M., Ritchie, P.A., Millar, C.D., Holland, B., Drummond, A.J., Baroni, C., 2002. Rates of evolution in ancient DNA from Adelie penguins. Science 295, 2270–2273.
Leonard, E.M., 1997. The relationship between glacial activity and sediment production: evidence from a 4450-year varve record of neoglacial sedimentation in Hector Lake, Alberta, Canada. J. Paleolimnol. 17, 319–330.
Leventer, A., Domack, E., Dunbar, R., Pike, J., Stickley, C., Maddison, E., Brachfeld, S., Manley, P., McClennen, C., 2006. Marine sediment record from the East Antarctic margin reveals dynamics of ice sheet recession. GSA Today 16, 4.
Lewan, M.D., Maynard, J.B., 1982. Factors controlling enrichment of vanadium and nickel in the bitumen of organic sedimentary-rocks. Geochim. Cosmochim. Acta 46, 2547–2560.
Li, C., Zhang, Y., Li, J., Kong, L., Hu, H., Pan, H., Xu, L., Deng, Y., Li, Q., Jin, L., Yu, H., Chen, Y., Liu, B., Yang, L., Liu, S., Zhang, Y., Lang, Y., Xia, J., He, W., Shi, Q., Subramanian, S., Millar, C.D., Meader, S., Rands, C.M., Fujita, M.K., Greenwold, M.J., Castoe, T.A., Pollock, D.D., Gu, W., Nam, K., Ellegren, H., Ho, S.Y.W., Burt, D.W., Ponting, C.P., Jarvis, E.D., Gilbert, M.T.P., Yang, H., Wang, J., Lambert, D.M., Wang, J., Zhang, G., 2014. Two Antarctic penguin genomes reveal insights into their evolutionary history and molecular changes related to the Antarctic environment. Gigascience 3.
Lynch, H.J., LaRue, M.A., 2014. First global census of the Adelie Penguin. Auk 131, 457–466.
Mackintosh, A.N., Verleyen, E., O'Brien, P.E., White, D.A., Jones, R.S., McKay, R., Dunbar, R., Gore, D.B., Fink, D., Post, A.L., Miura, H., Leventer, A., Goodwin, I., Hodgson, D.A., Lilly, K., Crosta, X., Golledge, N.R., Wagner, B., Berg, S., van Ommen, T.,

Zwartz, D., Roberts, S.J., Vyverman, W., Masse, G., 2014. Retreat history of the East Antarctic Ice Sheet since the Last Glacial Maximum. Quat. Sci. Rev. 100, 10–30.
McMinn, A., Heijnis, H., Harle, K., McOrist, G., 2001. Late-Holocene climatic change recorded in sediment cores from Ellis Fjord, eastern Antarctica. The Holocene 11, 291–300.
Milliken, K.T., Anderson, J.B., Wellner, J.S., Bohaty, S.M., Manley, P.L., 2009. High-resolution Holocene climate record from Maxwell Bay, South Shetland Islands, Antarctica. Geol. Soc. Am. Bull. 121, 1711–1725.
Nicol, S., Pauly, T., Bindoff, N.L., Wright, S., Thiele, D., Hosie, G.W., Strutton, P.G., Woehler, E., 2000. Ocean circulation off east Antarctica affects ecosystem structure and sea-ice extent. Nature 406, 504–507.
Nie, Y., Sun, L., Liu, X., Emslie, S.D., 2015. From warm to cold: migration of Adélie penguins within Cape Bird, Ross Island. Sci. Rep. 5.
Pickard, J., Adamson, D.A., Heath, C.W., 1986. The evolution of watts lake, Vestfold hills, east Antarctica, from marine inlet to fresh-water lake. Palaeogeogr. Palaeoclimatol. Palaeoecol. 53, 271–288.
Reimer, P.J., Bard, E., Bayliss, A., Beck, J.W., Blackwell, P.G., Ramsey, C.B., Buck, C.E., Cheng, H., Edwards, R.L., Friedrich, M., Grootes, P.M., Guilderson, T.P., Haflidason, H., Hajdas, I., Hatte, C., Heaton, T.J., Hoffmann, D.L., Hogg, A.G., Hughen, K.A., Kaiser, K.F., Kromer, B., Manning, S.W., Niu, M., Reimer, R.W., Richards, D.A., Scott, E.M., Southon, J.R., Staff, R.A., Turney, C.S.M., van der Plicht, J., 2013. Intcal13 and marine13 radiocarbon age calibration curves 0–50,000 years Cal Bp. Radiocarbon 55, 1869–1887.
Ritchie, P.A., Millar, C.D., Gibb, G.C., Baroni, C., Lambert, D.M., 2004. Ancient DNA enables timing of the Pleistocene origin and Holocene expansion of two Adélie penguin lineages in Antarctica. Mol. Biol. Evol. 21 (2), 240–248.
Roberts, D., McMinn, A., 1996. Relationships between surface sediment diatom assemblages and water chemistry gradients in saline lakes of the Vestfold Hills, Antarctica. Antarct. Sci. 8, 331–341.
Roberts, D., McMinn, A., 1998. A weighted-averaging regression and calibration model for inferring lakewater salinity from fossil diatom assemblages in saline lakes of the Vestfold hills: a new tool for interpreting Holocene lake histories in Antarctica. J. Paleolimnol. 19, 99–113.
Roberts, D., McMinn, A., 1999. A diatom-based palaeosalinity history of Ace Lake, Vestfold Hills, Antarctica. The Holocene 9, 401–408.
Roberts, S.J., Monien, P., Foster, L.C., Loftfield, J., Hocking, E.P., Schnetger, B., Pearson, E.J., Juggins, S., Fretwell, P., Ireland, L., Ochyra, R., Haworth, A.R., Allen, C.S., Moreton, S.G., Davies, S.J., Brumsack, H.-J., Bentley, M.J., Hodgson, D.A., 2017. Past penguin colony responses to explosive volcanism on the Antarctic Peninsula. Nat. Commun. 8, 14914.
Ropert-Coudert, Y., Kato, A., Meyer, X., Pellé, M., MacIntosh, A., Angelier, F., Chastel, O., Widmann, M., Arthur, B., Raymond, B., 2015. A complete breeding failure in an Adélie penguin colony correlates with unusual and extreme environmental events. Ecography 38, 111–113.
Rouff, A.A., 2012. Sorption of chromium with Struvite during phosphorus recovery. Environ. Sci. Technol. 46, 12493–12501.
Sands, M., Nicol, S., McMinn, A., 1998. Fluoride in Antarctic marine crustaceans. Mar. Biol. 132, 591–598.
Soevik, T., Braekkan, O.R., 1979. Fluoride in Antarctic krill (euphausia-superba) and Atlantic krill (meganyctiphanes-norvegica). J. Fish. Res. Board Can. 36, 1414–1416.
Southwell, C., Emmerson, L., 2013. Large-scale occupancy surveys in East Antarctica discover new Adelie penguin breeding sites and reveal an expanding breeding distribution. Antarct. Sci. 25, 531–535.
Southwell, C., Emmerson, L., McKinlay, J., Newbery, K., Takahashi, A., Kato, A., Barbraud, C., DeLord, K., Weimerskirch, H., 2015. Spatially extensive standardized surveys reveal widespread, multi-decadal increase in East Antarctic Ad'elie penguin populations. PLoS One 10.
Southwell, C., Emmerson, L., Takahashi, A., Barbraud, C., Delord, K., Weimerskirch, H., 2017. Large-scale population assessment informs conservation management for seabirds in Antarctica and the Southern Ocean: a case study of Adélie penguins. Global Ecol. Conserv. 9, 104–115.
Sprenk, D., Weber, M.E., Kuhn, G., Wennrich, V., Hartmann, T., Seelos, K., 2014. Seasonal changes in glacial polynya activity inferred from Weddell Sea varves. Clim. Past 10, 1239–1251.
Stenni, B., Buiron, D., Frezzotti, M., Albani, S., Barbante, C., Bard, E., Barnola, J.M., Baroni, M., Baumgartner, M., Bonazza, M., Capron, E., Castellano, E., Chappellaz, J., Delmonte, B., Falourd, S., Genoni, L., Iacumin, P., Jouzel, J., Kipfstuhl, S., Landais, A., Lemieux-Dudon, B., Maggi, V., Masson-Delmotte, V., Mazzola, C., Minster, B., Montagnat, M., Mulvaney, R., Narcisi, B., Oerter, H., Parrenin, F., Petit, J.R., Ritz, C., Scarchilli, C., Schilt, A., Schuepbach, S., Schwander, J., Selmo, E., Severi, M., Stocker, T.F., Udisti, R., 2011. Expression of the bipolar see-saw in Antarctic climate records during the last deglaciation. Nat. Geosci. 4, 46–49.
Stuiver, M., Reimer, P.J., 1993. Extended C-14 data-base and revised calib 3.0 C-14 age calibration program. Radiocarbon 35, 215–230.
Stuiver, M., Pearson, G.W., Braziunas, T., 1986. Radiocarbon age calibration of marine samples back to 9000 Cal Yr Bp. Radiocarbon 28, 980–1021.
Sun, L.G., Xie, Z.Q., Zhao, J.L., 2000. Palaeoecology - a 3,000-year record of penguin populations. Nature 407, 858.
Sun, L.G., Zhu, R.B., Liu, X.D., Xie, Z.Q., Yin, X.B., Zhao, S.P., Wang, Y.H., 2005. HCl-soluble Sr-87/Sr-86 ratio in sediments impacted by penguin or seal excreta as a proxy for historical population size in the maritime Antarctic. Mar. Ecol. Prog. Ser. 303, 43–50.
Tatur, A., Keck, A., 1990. Phosphates in ornithogenic soils of the maritime Antarctic. In: Proceedings of the NIPR Symposium on Polar Biology. 3. pp. 133–150.
Taylor, F., Whitehead, J., Domack, E., 2001. Holocene paleoclimate change in the Antarctic Peninsula: evidence from the diatom, sedimentary and geochemical record. Mar. Micropaleontol. 41, 25–43.
Verleyen, E., Hodgson, D.A., Sabbe, K., Vyverman, W., 2004. Late Quaternary deglaciation and climate history of the Larsemann Hills (East Antarctica). J. Quat. Sci. 19, 361–375.
Verleyen, E., Hodgson, D.A., Milne, G.A., Sabbe, K., Vyverman, W., 2005. Relative sea-level history from the Lambert Glacier region, East Antarctica, and its relation to deglaciation and Holocene glacier readvance. Quat. Res. 63, 45–52.
Verleyen, E., Hodgson, D.A., Sabbe, K., Cremer, H., Emslie, S.D., Gibson, J., Hall, B., Imura, S., Kudoh, S., Marshall, G.J., McMinn, A., Melles, M., Newman, L., Roberts, D., Roberts, S.J., Singh, S.M., Sterken, M., Tavernier, I., Verkulich, S., Van de Vyver, E., Van Nieuwenhuyze, W., Wagner, B., Vyverman, W., 2011. Post-glacial regional climate variability along the East Antarctic coastal margin-evidence from shallow marine and coastal terrestrial records. Earth Sci. Rev. 104, 199–212.
Wagner, B., Cremer, H., Hultzsch, N., Gore, D.B., Melles, M., 2004. Late Pleistocene and Holocene history of Lake Terrasovoje, Amery Oasis, East Antarctica, and its climatic and environmental implications. J. Paleolimnol. 32, 321–339.
Wagner, B., Hultzsch, N., Melles, M., Gore, D.B., 2007. Indications of holocene sea-level rise in Beaver Lake, East Antarctica. Antarct. Sci. 19, 125–128.
Wang, J., Wang, Y., Wang, X., Sun, L., 2007. Penguins and vegetations on Ardley Island, Antarctica: evolution in the past 2,400 years. Polar Biol. 30, 1475–1481.
Weber, M.E., Clark, P.U., Ricken, W., Mitrovica, J.X., Hostetler, S.W., Kuhn, G., 2011. Interhemispheric ice-sheet synchronicity during the last glacial maximum. Science 334, 1265–1269.
Wilson, P.R., Ainley, D.G., Nur, N., Jacobs, S.S., Barton, K.J., Ballard, G., Comiso, J.C., 2001. Adelie penguin population change in the pacific sector of Antarctica: relation to sea-ice extent and the Antarctic Circumpolar Current. Mar. Ecol. Prog. Ser. 213, 301–309.
Yang, L., Sun, L., Emslie, S.D., Xie, Z., Huang, T., Gao, Y., Yang, W., Chu, Z., Wang, Y., 2018. Oceanographic mechanisms and penguin population increases during the Little Ice Age in the southern Ross Sea, Antarctica. Earth Planet. Sci. Lett. 481, 136–142.
Younger, J., Emmerson, L., Southwell, C., Lelliott, P., Miller, K., 2015. Proliferation of East Antarctic Ad'elie penguins in response to historical deglaciation. BMC Evol. Biol. 15.
Younger, J.L., Emmerson, L.M., Miller, K.J., 2016. The influence of historical climate changes on Southern Ocean marine predator populations: a comparative analysis. Glob. Chang. Biol. 22, 474–493.
Yuan, L., Sun, L., Long, N., Xie, Z., Wang, Y., Liu, X., 2010. Seabirds colonized Ny-Ålesund, Svalbard, Arctic ~9,400 years ago. Polar Biol. 33, 683–691.